INTERNATIONAL JOURNAL OF REFRIGERATION 87 (2018) 164–171

Available online at www.sciencedirect.com

ScienceDirect

journal homepage: www.elsevier.com/locate/ijrefrig

Short Report

A semi-empirical model for predicting frost accretion on hydrophilic and hydrophobic surfaces

Christian J.L. Hermes [a,*], *Andrew D. Sommers* [b], *Colton W. Gebhart* [b], *Valter S. Nascimento Jr.* [c]

[a] *POLO Research Laboratories, Department of Mechanical Engineering, Federal University of Santa Catarina, Florianópolis, SC 88040535, Brazil*

[b] *Department of Mechanical and Manufacturing Engineering, Miami University, 56 Garland Hall, 650 East High Street, Oxford, OH 45056, USA*

[c] *Post-Graduation Program in Materials Science and Engineering, Federal University of Paraná, Curitiba, PR 81530000, Brazil*

ARTICLE INFO

Article history:
Received 23 August 2017
Received in revised form 20 September 2017
Accepted 26 September 2017
Available online 6 October 2017

Keywords:
Frost
Growth
Correlation
Surface
Free convection

ABSTRACT

A first-principles model was used together with experimental data obtained in-house to validate a semi-empirical modeling approach for predicting frost accretion on hydrophilic and hydrophobic substrates. An algebraic expression for the frost thickness as a function of the time, the modified Jakob number, the humidity gradient, and the surface contact angle was devised from frost formation theory. At this stage, the correlation was fitted to 956 experimental data points for natural convection conditions spanning different surface temperatures and supercooling degrees, with the modified Jakob number ranging from 0.79 to 1.30, and contact angles ranging from 45° (hydrophilic) to 160° (hydrophobic). When compared to the experimental data for the frost thickness, the proposed semi-empirical model showed errors within ±15% bounds, and an average predictive error of 11.7%. Since the model carries the contact angle as an independent parameter, a sensitivity analysis of the frost growth rate in relation to it is also reported.

Modélisation semi-empirique pour prédire l'accrétion de givre sur des surfaces hydrophiles et hydrophobes

Mots clés : Givre ; Croissance ; Corrélation ; Surface ; Convection libre

* *Corresponding author.* POLO Research Laboratories, Department of Mechanical Engineering, Federal University of Santa Catarina, Florianópolis, SC 88040535, Brazil.
E-mail address: hermes@polo.ufsc.br (C.J.L. Hermes).

https://doi.org/10.1016/j.ijrefrig.2017.09.022

Nomenclature

Roman

D	diffusivity of water vapor in air [$m^2\ s^{-1}$]
DCA	dynamic contact angle [rad]
i_{sv}	latent heat of sublimation (=2.83×10^6) [$J\ kg^{-1}$]
Ja	modified Jakob number
L	plate length [m]
Le	Lewis number
m	mass flux [$kg\ m^{-2}\ s^{-1}$]
p	pressure [Pa]
Ra	Rayleigh number
Sh	Sherwood number
T	temperature [°C]
t	time [s]
u	velocity [$m\ s^{-1}$]

Greek

δ	frost thickness [m]
ϕ	relative humidity
θ	static contact angle [rad]
ρ	density [$kg\ m^{-3}$]
ρ_f	frost density [$kg\ m^{-3}$]
ω	humidity ratio [$kg_v\ kg^{-1}$]

Subscripts

a	Moist air
f	Frost
i	Ice
s	Frost surface
sat	Saturation
w	Plate surface

Introduction

In most refrigeration applications, evaporator frosting is an undesirable aspect as it depletes the cooling capacity by adding an extra thermal insulation layer, and additionally it increases the air-side pressure drop by reducing the free flow passage, thus requiring the compressor to run longer cycles to promote the same desired cooling effect. In modern systems, however, air-supplied evaporators are designed to be robust to frost clogging either by choosing a proper defrost strategy (e.g., defrost heater type, power, and positioning; see Melo et al., 2013) or managing an optimal defrost cycle (i.e., time between defrost operations; see Radcenco et al., 1995). For this purpose, simulation models for evaporator frosting prediction have been advanced and improved in the past few decades. Silva et al. (2017), for instance, brings about a comprehensive review of the most influencing simulation models available in the open literature. Those models were devised aiming not only at improving accuracy but also at accounting for new features, such as multidimensional frost distribution (Knabben et al., 2011) and fan-coil hydrodynamic coupling (Silva et al., 2011).

In general, as a rule of thumb, frost formation models are initially devised for simplified geometries (as flat plates or parallel-plate channels) before being implemented for more complex geometries, such as fin-and-tube heat exchangers (Popovac et al., 2015). Table 1 summarizes some of the key simulation models developed for simplified geometries since the early 1980s. It is important to note that, although most models account for the temperature and humidity variations within the frost layer (which is typically modeled as a porous medium), the air-frost interface condition has been treated as saturated until recent times (El Cheikh and Jacobi, 2014; Loyola et al., 2014), despite the recognized importance of the supersaturation degree in the frost nucleation and accretion processes (Hermes et al., 2009; Piucco et al., 2008) and its influence on model accuracy.

Table 1 – Summary of some influential studies on frost growth modeling.

Author	Origin	Porous Medium	Geometry	Initial condition		Thermal Conductivity	Air-Frost Interface
				Thickness [mm]	Density [$kg\ m^{-3}$]	Model	
O'Neal (1982)	USA	Yes	Channel	0.05	40	Sanders (1974)	Saturated
Sami and Duong (1989)	Canada	Yes	Flat plate	–	–	Yonko and Sepsy (1967)	Saturated
Tao et al. (1993)	Canada	No	Flat plate	0.1	92.84	Their own	Saturated
Le Gall et al. (1997)	France	Yes	Flat plate	0.1	25	Auracher (1986)	Saturated
Lee et al. (1997)	S. Korea	No	Flat plate	–	–	Lee et al. (1997)	Saturated
Luer & Beer (2000)	Germany	Yes	Channel	0	various	Auracher (1986)	Saturated
Cheng and Cheng (2001)	China	No	Flat plate	–	Hayashi et al. (1977)	Brian et al. (1969)	Saturated
Na and Webb (2004)	USA	Yes	Flat plate	0.02	30	Sanders (1974)	Saturated
Hermes et al. (2009)	Brazil	Yes	Flat plate	0.001	their own	Lee et al. (1997)	Saturated
Kandula (2011)	USA	Yes	Flat plate	0	their own	Kandula (2011)	Saturated
Cui et al. (2011)	China	Yes	Channel	0	nucleation model	Cubic lattice model	Saturated
Hermes (2012)	Brazil	Yes	Flat plate	0.001	their own	Lee et al. (1997)	Saturated
Loyola et al. (2014)	Brazil	Yes	Channel	0.001	Nascimento et al. (2015)	Hermes (2012)	Supersaturated
El Cheikh and Jacobi (2014)	USA	Yes	Flat plate	0.0001	40	O'Neal and Tree (1985)	Supersaturated

Another issue that has gained recent attention is the influence of the surface microscopic characteristics (i.e. contact angle, roughness, etc.) on the macroscopic properties of the frosted media. For instance, Sommers et al. (2016) analyzed the properties of a growing frost layer for surfaces of varying wettability to determine the influence that the surface energy exerts on the frost thickness and density. In a follow-up study by the same group (Sommers et al., (2017b), a semi-empirical frost density correlation was proposed being able to predict more than 93% of the data to within a 20% error band and is proposed for use on surfaces with contact angles ranging from 45° to 160°, relative humidity from 0.40 to 0.80, and plate temperatures from –13 °C to –5 °C under natural convection conditions.

Muntaha et al. (2016) proposed a model for frost buildup on periodic rectangular microgroove surfaces, which takes the effect of surface wettability into account by considering the variation of the initial frost thickness and density which result from the variation of the surface micro-roughness. It is worth noting that the model itself carries no explicit information about the surface characteristics, which have been incorporated into it by means of artificial initial conditions from experimental data obtained elsewhere (Rahman and Jacobi, 2013). The paper focused on micro-roughness, and the range of contact angles for which the model is applicable has not been reported.

In addition to the first-principles models summarized in Table 1, various empirical and semi-empirical models for predicting the frost thickness have also been proposed in the literature (Iragorry et al., 2004). Schneider (1978), for instance, proposed the following algebraic expression for the time-evolution of the frost thickness,

$$\delta = 0.465\left[\frac{k_i}{i_{sv}\rho_i}(T_s - T_w)t\right]^{1/2}(t[h])^{0.03}(T_s - T_w)^{-0.01}\left(\frac{p_a - p_{sat,s}}{p_{sat,a} - p_{sat,s}}\right)^{1/4}\left(1 + 0.052\frac{T_a - T_m}{T_m - T_w}\right) \quad (1)$$

where k_i and ρ_i are the thermal conductivity and density of ice, i_{sv} is the latent heat of sublimation, and T_m is the melting point of ice. Eq. (1) is valid for forced convection (4000< Re <32000), -30< T_w <-5°C, 5< T_a<15 °C, and 60< t <480 min. Shin et al. (2003) proposed the following empirical correlation for the frost thickness:

$$\delta = (0.0852 + 0.00134 \cdot DCA)\,t^{(0.6954 - 0.00154 \cdot DCA)} \quad (2)$$

where DCA is the dynamic contact angle. Although this model accounts for surface wettability, it should be pointed out that this correlation was developed for a very specific set of operating conditions (T_w = –22 °C, T_a = 12°C, RH = 48%) and for hydrophilic surfaces only (DCA~23-88°), and thus does not have broad applicability.

To the authors' best knowledge, there exists a need in the literature for a model capable of predicting the frost accretion on substrates spanning a wide range of contact angles. The present paper fills this gap by presenting and validating a semi-empirical algebraic model for frost accretion on both hydrophilic and hydrophobic substrates. Since the model carries the contact angle as an independent parameter, a sensitivity analysis of the frost growth rate in relation to the contact angle is also reported.

Formulation

Most frost formation models have been formulated based on the following assumptions: quasi-steady, one-dimensional mass and heat diffusion within the frost layer; uniform frost thickness; and the Lewis analogy is applicable. Therefore, both frost growth and densification processes can be represented by the overall mass balance in the frost layer represented in Fig. 1, yielding

$$\delta\frac{d\rho_f}{dt} + \rho_f\frac{d\delta}{dt} = m \quad (3)$$

where the first term on the left-hand side represents the densification of the frost layer as a function of time, and the second term represents the frost layer growth rate. It has been demonstrated in the literature (Nascimento et al., 2015; Negrelli et al., 2016) that, for low velocities, the frost mass behaves linearly with time, M~t, as depicted in Fig. 2, in such a way that the mass flux of water vapor, m, is constant over time. Additionally, the frost density can be expressed in the following form:

$$\rho_f = \rho_i C Ja^{-n}\sqrt{t} \quad (4)$$

where C may be either a constant (Hermes et al., 2014) or a function of the surface contact angle and the relative humidity (Sommers et al., 2017b), n = 3/2 for flat surfaces (Hermes et al., 2014) and n = 3/4 for parallel plate channels (Nascimento

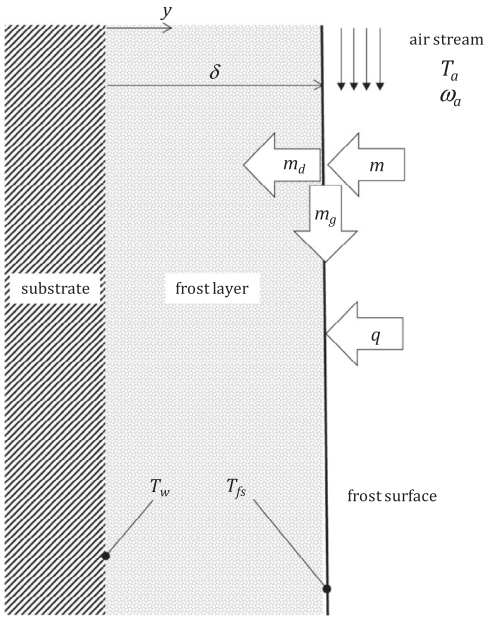

Fig. 1 – Physical model for frost growth and densification over a vertical flat surface under natural convection.

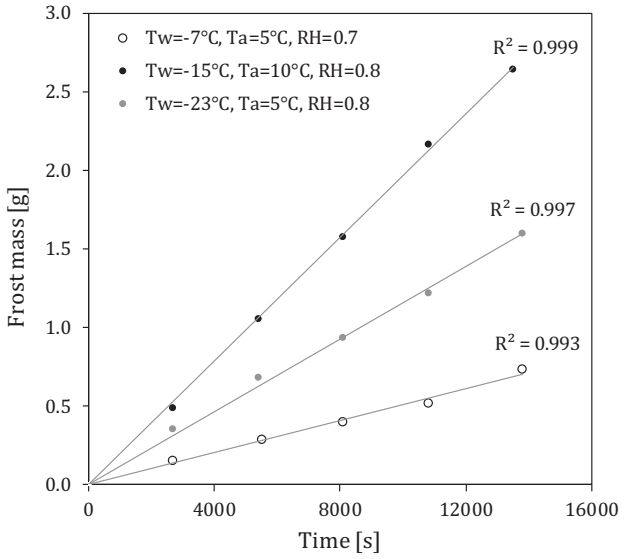

Fig. 2 – Experimental data showing the linear relationship ($R^2 > 0.99$) between the frost mass and the time for low air velocities (Data from Negrelli et al., 2016).

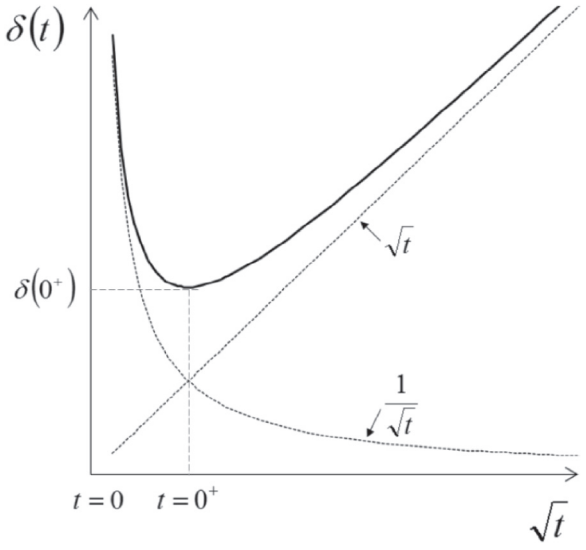

Fig. 3 – Schematic illustration of the asymptotes in Eq. (7).

et al., 2015), respectively, and $Ja=(c_p/i_{sv})(T_{dew}-T_w)/(\omega_{air}-\omega_{sat,w})$ is the modified Jakob number, as introduced by Hermes et al. (2014). Substituting the time-derivative of Eq. (4) into Eq. (3), one can obtain the following ordinary-differential equation for the frost growth rate:

$$\frac{d\delta}{dt}+\frac{\delta}{2t}=\frac{m}{\rho_i C Ja^{-n}\sqrt{t}} \tag{5}$$

where $m/\rho_i C Ja^{-n}$ is constant over time. The analytical solution of Eq. (5) yields the following expression for the time evolution of the frost thickness:

$$\delta(t)=\frac{m}{\rho_i C Ja^{-n}}\sqrt{t}+\frac{b}{\sqrt{t}} \tag{6}$$

To further improve the model accuracy, it is convenient to write the mass flow rate as $m=\rho_a D\Delta\omega Sh/L$, where D is the water vapor diffusivity in air [$m^2\ s^{-1}$], and L is the plate length in the flow direction. Under forced convection conditions, the Sherwood number scales with both Reynolds and Prandtl numbers, $Sh\sim Re^m Pr^{1/3}$, where $m \approx 1/2$ for laminar and 4/5 for turbulent flows. On the other hand, under natural draft conditions the Sherwood number scales with Rayleigh and Lewis numbers, $Sh\sim Ra^m Le^{1/3}$, where $Le\approx 1$ for moist air under atmospheric conditions, and $m \approx 1/4$ for laminar and 1/3 for turbulent flows. Therefore, Equation (6) can be rewritten as

$$\delta(t)=a\left(\frac{\rho_a}{\rho_i}\right)\left(\frac{D\Delta\omega}{L}\right)ShJa^n\sqrt{t}+\frac{b}{\sqrt{t}} \tag{7}$$

where the coefficients a [$s^{1/2}$] and b [$m\ s^{1/2}$], and exponents m and n (≈3/4~3/2) must be best-fitted to the experimental data to come out with a semi-empirical correlation for the time-evolution of the frost thickness, δ(t). One may expect both the a and b coefficients to be functions of the contact angle, the former due to the surface effects on the density and the latter to account for the initial condition $\delta(t = 0^+)$ for the frost thickness, where $t = 0^+$ denotes the time when the frosting process becomes macroscopic so that the proposed model – which has been based on the continuum – is applicable.

An inspection of Eq. (7) reveals two asymptotes in the time domain, one related to the first term ($\sim t^{1/2}$) and another to the second term ($\sim t^{-1/2}$) both on the right-hand side of the equation, the former related to frost growth and the latter to frost decay over time, as depicted in Fig. 3. On thermodynamic grounds, however, no frost decay is possible for a positive mass gradient ($D\Delta\omega/L$) such that the model must be applicable from the time when $d\delta/dt=0$ (i.e., $t = 0^+$) on. Therefore, taking the derivative of Eq. (7) with respect to time and setting it equal to zero, the initial condition for the macroscopic frost growth model can be calculated as follows:

$$t_{0^+}=\sqrt{\frac{b}{a\left(\frac{\rho_a}{\rho_i}\right)\left(\frac{D\Delta\omega}{L}\right)ShJa^n}} \tag{8}$$

Substituting Eq. (8) into Eq. (7) yields the following expression for the initial condition for the frost growth model:

$$\delta_{0^+}=b^{1/4}\left[a\left(\frac{\rho_a}{\rho_i}\right)\left(\frac{D\Delta\omega}{L}\right)ShJa^n\right]^{3/4}+b^{3/4}\left[a\left(\frac{\rho_a}{\rho_i}\right)\left(\frac{D\Delta\omega}{L}\right)ShJa^n\right]^{1/4} \tag{9}$$

Discussion

The correlation was derived using natural convection data from Sommers et al. (2017a) for three different surfaces each having a different static equilibrium contact angle: a baseline surface S1 (θ = 81.9°), a hydrophilic surface S3 (θ = 45.3°), and a hydrophobic surface S2 (θ = 158.9°). Details about the various operating

Table 2 – Summary of experimental frost growth conditions.

No.	Surface	T_a (°C)*	T_w (°C)*	RH**	Ja
1	S1	21.9	–8.3	80%	0.82
2	S1	21.8	–6.3	80%	0.79
3	S1	18.9	–12.2	60%	1.18
4	S1	22.7	–10.4	60%	1.00
5	S1	22.6	–8.1	40%	1.17
6	S1	23.1	–10.2	40%	1.22
7	S1	23.0	–12.6	40%	1.30
8	S1	20.4	–8.0	60%	1.01
9	S1	18.0	–7.2	80%	0.92
10	S1	22.6	–5.3	60%	0.88
11	S2	21.6	–8.5	60%	0.99
12	S2	20.5	–8.5	80%	0.87
13	S2	23.5	–7.4	40%	1.12
14	S2	22.5	–10.5	40%	1.26
15	S2	23.8	–11.7	40%	1.24
16	S2	18.6	–10.2	60%	1.14
17	S2	20.2	–11.8	60%	1.12
18	S2	23.2	–11.7	40%	1.27
19	S2	21.6	–12.3	60%	1.08
20	S2	23.6	–7.5	40%	1.12
21	S2	19.9	–8.9	80%	0.90
22	S3	20.4	–10.1	80%	0.91
23	S3	20.5	–11.1	80%	0.92
24	S3	22.9	–9.7	60%	0.97
25	S3	23.0	–7.5	60%	0.91
26	S3	20.8	–7.0	80%	0.83
27	S3	19.0	–9.4	60%	1.10
28	S3	21.9	–11.3	60%	1.05

* test average.
** ± 2-3% (typical).

conditions that were examined can be found in Table 2. Additional details about the surfaces and the experimental setup including sample images of the frost layer can be found in Sommers et al. (2016).

Using the data associated with the 28 cases for natural convection conditions shown in Table 2 (N > 950), a multiple regression analysis was performed to find the best-fit values for the correlation form shown in Eq. (7). In performing this least-squares error analysis, it was discovered that the dependence on Sherwood number (Sh) was found to be small for natural convection conditions, as $5.3\times10^7<Ra<1.9\times10^8$ in these experiments, so this term was removed from the correlation. The density ratio (ρ_a/ρ_i) was also removed from Eq. (7), as it is fairly constant in the temperature range considered (see Table 2). Next, the following correlation form was tried:

$$\delta(t) = C_1\left(\frac{D\Delta\omega}{L}\right)Ja^n\sqrt{t} + \frac{C_2 e^{k\theta}}{\sqrt{t}} \tag{10}$$

The form of the numerator in the second term (the former b coefficient shown in Eq. 7) was chosen because of the dependence of the frost layer height on surface wettability, especially at small times (i.e. $t\sim0^+$). It should be noted that this term depends on the static contact angle of the surface and was selected following experimentation with various functional forms. Multiple regression analysis was then performed again to find the best-fit values for C_1, C_2, n and k. The exponents n and k were found to be very close to 1.5 and 0.5, respectively. Thus, these coefficients were fixed at these values, and the regression analysis was performed a final time to find the new best-fit values for C_1 and C_2. The following expression for the frost thickness was arrived at

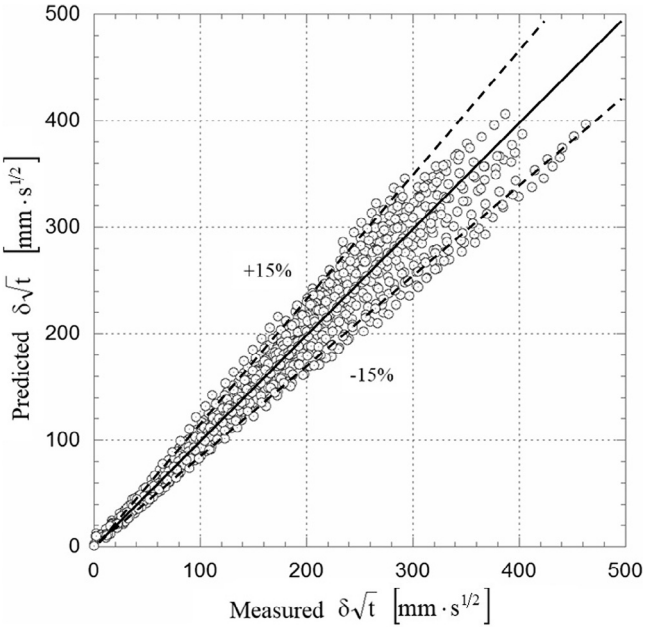

Fig. 4 – Comparison between experimental and predicted frost thickness values for all data.

$$\delta(t) = 1.26\times10^4\left(\frac{D\Delta\omega}{L}\right)Ja^{3/2}\sqrt{t} + \frac{0.53e^{\theta/2}}{\sqrt{t}} \tag{11}$$

where the surface contact angle θ is given in radians, time t is in seconds, and thickness δ in mm. It should be pointed out that the least-squares regression analysis derived value of n = 3/2 for the modified Jakob number agrees well with earlier studies (Hermes et al., 2014). It should be emphasized that Eq. (11) is valid for $t>0^+$ as the second term blows up as $t\to0$.

When compared to the experimental frost thickness, the new correlation predicted 94.8% of the data to within ±20% of the measured value. Stated another way, the average predictive error for all the non-zero data was 11.7% (N = 930). Predicting early frost thickness values is quite difficult due to the rapid changes in the frost layer for $t<0^+$, when both heat and mass transport are not ruled by diffusion. It should be pointed out that this difficulty is true for all frost thickness models (not just this model) but is not of great consequence since longer time frost thickness values are typically of greater importance from an application point of view. Overall, the new proposed correlation predicted 92.1% of the baseline data, 98.9% of the hydrophobic data, and 92.5% of the hydrophilic data to with ±20% of the experimental frost thickness value.

Fig. 4 shows a comparison between the predicted and experimental frost thickness with ±15% error bounds. Fig. 5 shows the measured frost thickness as a function of time on the three test surfaces compared against the new correlation for different operating conditions. Good agreement is noted in all the cases.

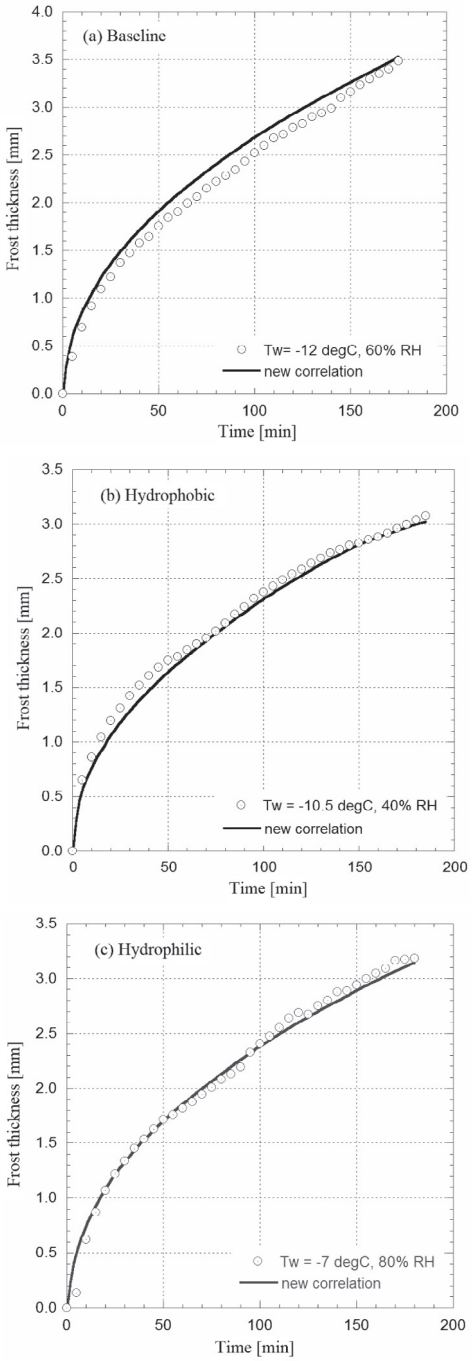

Fig. 5 – Predicted frost thickness as a function of time versus the experimental data for the three surfaces under different operating conditions: (a) baseline surface S1 (θ = 81.9°), (b) hydrophobic surface S2 (θ = 158.9°), and (c) hydrophilic surface S3 (θ = 45.3°).

Based on Eqs. (8), (9) and (11), one can show that the initial conditions for the macroscopic frost growth model can be calculated as follows:

$$t_{0^+} = 6.49\times10^{-3}\left(\frac{D\Delta\omega}{L}\right)^{-1/2} Ja^{-3/4}e^{\theta/4} \tag{12}$$

Table 3 – Initial conditions calculated from Eqs. (12) and (13) for different Ja and θ (Δω/L = –0.1 m^{-1}).

θ	Ja	t (0$^+$) [s]	δ (0$^+$) [mm]
45	0.5	8.5	0.30
90	0.5	10.4	0.40
135	0.5	12.7	0.52
45	1	5.1	0.42
90	1	6.2	0.54
135	1	7.5	0.71
45	1.5	3.8	0.51
90	1.5	4.6	0.66
135	1.5	5.6	0.86

$$\delta_{0^+} = 1014.7\left(\frac{D\Delta\omega}{L}\right)^{3/4} Ja^{9/8}e^{\theta/8} + 6.58\left(\frac{D\Delta\omega}{L}\right)^{1/4} Ja^{3/8}e^{3\theta/8} \tag{13}$$

Table 3 compares the values obtained from Eqs. (12) and (13) for Ja varying from 0.5 to 1.5, and θ ranging from 45° to 135°. One can see in Table 3 that the highest initial calculated time (12.7 s) was observed for the highest θ and lowest Ja, being more sensitive to the latter. Such a value is quite small in comparison to the whole time-domain (~7200 s). Table 3 also shows the calculated values for the initial frost thickness calculated using Eq. (13). Unlike the initial times, which represent a small fraction (~10^{-5} %) of the whole period, calculated values for the initial frost thicknesses of up to 0.86 mm were found (in this case, for the highest θ and Ja), which represent ~10-25% of the total thickness. An inspection of Table 3 also reveals that the initial thickness is quite sensitive to the contact angle, varying by 0.25 mm from 45° to 135°. This can therefore be quite important when trying to model the growth of the frost layer accurately. Hence, there are two options for predicting the frost thickness over time, namely: (i) the use of Eq. (11) as is, or (ii) the use of Eq. (13) together with one of the simulation models discussed in Table 1.

It is noted that the first term on the right-hand side of Eq. (11) is ruled by the modified Jakob number, whereas the second one is driven by the contact angle, θ. The sensitivity of the frost thickness in relation to these two parameters relies on the derivatives of δ with regard to Ja and θ, which can be calculated as follows in their semi-normalized form:

$$Ja\left.\frac{\partial\delta}{\partial Ja}\right|_{\theta} = \frac{3C_1}{2}\left(\frac{D\Delta\omega}{L}\right)Ja^{3/2}\sqrt{t} \tag{14}$$

$$\theta\left.\frac{\partial\delta}{\partial\theta}\right|_{Ja} = \frac{C_2}{2}\frac{\theta e^{\theta/2}}{\sqrt{t}} \tag{15}$$

Fig. 6 illustrates Eqs. (14) and (15) for Ja = 1, θ = 90° and Δω/L = 0.1 m^{-1}. One can see in Fig. 6, which shows the relative variation produced by θ and Ja on δ, that the second term (related to θ) plays a dominant role in the early stages of frost formation (see dashed line), being overtaken by the first term (related to Ja, solid line) after a little while. The θ-term decreases whereas the Ja-term increases asymptotically with $\sqrt{t}$, the latter being dominant most of the time. It is clear from Fig. 6 that the contact angle plays a minor role on the macroscopic frost thickness,

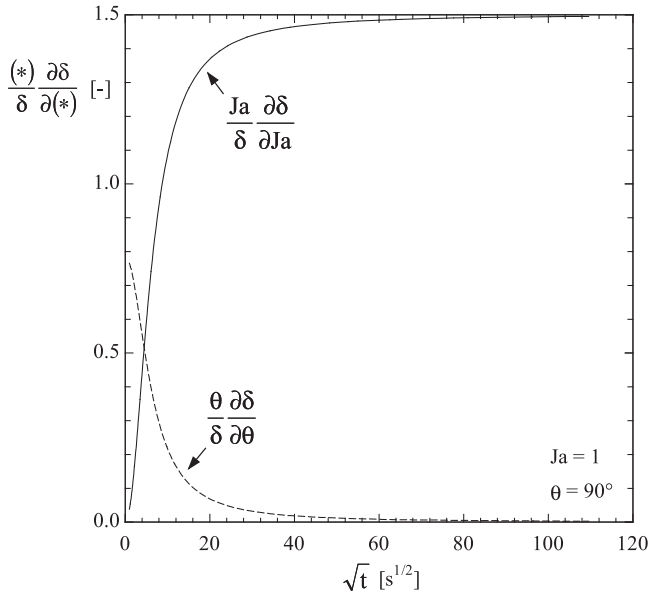

Fig. 6 – Frost thickness sensitivity to the modified Jakob number and the static contact angle.

whereas the modified Jakob number governs the frost growth process. An inspection of Fig. 6 together with Table 3 reveals that the contact angle effect is more pronounced in the early stages of frost formation for lower modified Jakob numbers.

Conclusions

A first-principles model was considered in conjunction with in-house experimental data to put forward a semi-empirical correlation for predicting the frost accretion on hydrophilic and hydrophobic substrates under natural draft conditions. An algebraic expression for the frost thickness as a function of the time, the modified Jakob number, the humidity gradient, and the surface contact angle was formulated. When compared to experimental data for the frost thickness, the proposed semi-empirical model showed an average predictive error of 11.7%. An inspection of the time-scale of the proposed correlation revealed that the initial time (in which the macroscopic approach is applicable) represents a small fraction (about 10^{-5} %) of the whole period, so that it may be set to zero. In contrast, the initial frost thickness represents about 10-25% of the total thickness, becoming important to ensure model accuracy. A sensitivity analysis revealed that the contact angle plays a relatively minor role on the macroscopic frost thickness, whereas the modified Jakob number dominates the frost accretion process. A similar model for frost build-up on flat surfaces under forced convection conditions is under development, and will be subject matter for a further publication.

Acknowledgments

A. Sommers and C. Gebhart gratefully acknowledge E. Caraballo, A. Napora, N. Truster, A. Riechman, and N. Schmiesing at Miami University for their help and assistance during the early stages of this project. V. Nascimento Jr. is thankful to the CAPES Agency, Government of Brazil, for supporting his doctorate at the Federal University of Paraná. C. Hermes duly acknowledges the financial support from the Brazilian Government funding agency CNPq (Grant No. 441603/2014-9).

REFERENCES

Auracher, H., 1986. Effective thermal conductivity of frost. In: Proceedings of the International Symposium of Heat and Mass Transfer in Refrigeration Cryogenics, Dubrovnik. pp. 285–302.

Brian, P.L.T., Reid, R.C., Brazinsky, I., 1969. Cryogenic frost properties. Cryogenic Technol. 10/11, 205–212.

Cheng, C.H., Cheng, Y.C., 2001. Predictions of frost growth on a cold plate in atmospheric air. Int. Commun. Heat Mass Transfer 28, 953–962.

Cui, J., Li, W.Z., Liu, Y., Jiang, Z.Y., 2011. A new time- and space-dependent model for predicting frost formation. App. Therm. Eng. 31, 447–457.

El Cheikh, A., Jacobi, A., 2014. A mathematical model for frost growth and densification on flat surfaces. Int. J. Heat Mass Transfer 77, 604–611.

Hayashi, Y., Aoki, A., Adashi, S., Hori, K., 1977. Study of frost properties correlating with frost formation types. ASME J. Heat Transfer 99, 239–245.

Hermes, C.J.L., 2012. An analytical solution to the problem of frost growth and densification on flat surfaces. Int. J. Heat Mass Transfer 55, 7346–7351.

Hermes, C.J.L., Piucco, R.O., Melo, C., Barbosa, J.R., Jr., 2009. A study of frost growth and densification on flat surfaces. Exp. Ther. Fluid Sci. 33, 371–379.

Hermes, C.J.L., Loyola, F.R., Nascimento, V.S., 2014. A semi-empirical correlation for the frost density. Int. J. Refrigeration 46, 100–104.

Iragorry, J., Tao, Y.-X., Jia, S., 2004. A critical review of properties and models for frost formation analysis. HVAC&R Res 10, 393–420.

Kandula, M., 2011. Frost growth and densification in laminar flow over flat surfaces. Int. J. Heat Mass Transfer 54, 3719–3731.

Knabben, F.T., Hermes, C.J.L., Melo, C., 2011. In-situ study of frosting and defrosting processes in tube-fin evaporators of household refrigerating appliances. Int. J. Refrigeration 34, 2031–2041.

Le Gall, R., Grillot, J.M., Jallut, C., 1997. Modelling of frost growth and densification. Int. J. Heat Mass Transfer 40, 3177–3187.

Lee, K.S., Kim, W.S., Lee, T.H., 1997. A one-dimensional model for frost formation on a cold flat surface. Int. J. Heat Mass Transfer 40, 4359–4365.

Loyola, F.R., Nascimento, V.S., Hermes, C.J.L., 2014. Modeling of frost build-up on parallel-plate channels under supersaturated air-frost interface conditions. Int. J. Heat Mass Transfer 79, 790–795.

Luer, A., Beer, H., 2000. Frost deposition in a parallel plate channel under laminar flow conditions. Int. J. Therm. Sci. 39, 85–95.

Melo, C., Knabben, F.T., Pereira, P.V., 2013. An experimental study on defrost heaters applied to frost-free household refrigerators. Appl. Therm. Eng. 51, 239–245.

Muntaha, M.A., Haider, M.M., Rahman, M.A., 2016. Modelling of frost formation and growth on microstructured surface. Int. Conf. Mech. Eng., AIP Conference Proceedings 1754, doi:10.1063/1.4958433. 050042, 7 pp.

Na, B., Webb, R., 2004. New model for frost growth rate. Int. J. Heat Mass Transfer 47, 925–936.
Nascimento, V.S., Loyola, F.R., Hermes, C.J.L., 2015. A study of frost build-up on parallel plate channels. Exp. Ther. Fluid Sci. 60, 328–336.
Negrelli, S., Nascimento, V.S., Hermes, C.J.L., 2016. A study of the effective thermal conductivity of frost formed on parallel plate channels. Exp. Ther. Fluid Sci. 78, 301–308.
O'Neal, D.L., 1982. The effects of frost formation on the performance of a parallel plate heat exchanger. PhD thesis, Department of Mechanical Engineering, Purdue University – West Lafayette-IN, USA.
O'Neal, D.L., Tree, D.R., 1985. A review of frost formation in simple geometries. ASHRAE Trans. 91, 267–281.
Piucco, R.O., Hermes, C.J.L., Melo, C., Barbosa, J.R., Jr., 2008. A study of frost nucleation on flat surfaces. Exp. Ther. Fluid Sci. 32, 1710–1715.
Popovac, M., Seichter, S., Benovsky, P., Fleckl, T., Reichl, C., Numerical analysis of the frosting performance of the air side of a heat pump, International Congress of Refrigeration, Yokohama, Japan, ID 28, 2015.
Radcenco, V., Vargas, J.V.C., Bejan, A., Lim, J.S., 1995. Two design aspects of defrosting refrigerators. Int. J. Refrigeration 18, 76–86.
Rahman, M.A., Jacobi, A.M., 2013. Effects of microgroove geometry on the early stages of frost formation and frost properties. Appl. Therm. Eng. 56, 91–100.
Sami, S.M., Duong, T., 1989. Mass and heat transfer during frost growth. ASHRAE Trans. 158–165.
Sanders, C.T., 1974. Frost formation: the influence of frost formation and defrosting on the performance of air coolers (PhD thesis). Dept. of Mechanical, Maritime and Materials Engineering, TU Delft, The Netherland.
Schneider, H.W., 1978. Equation of the growth rate of frost forming on cooled surfaces. Int. J. Heat Mass Transfer 21, 1019–1024.
Shin, J., Tikhonov, A.V., Kim, C., 2003. Experimental study on frost structure on surfaces with different hydrophilicity: density and thermal conductivity. J. Heat Transfer 125, 84–94.
Silva, D.L., Hermes, C.J.L., Melo, C., 2011. First-principles simulation of frost accumulation on fan-supplied tube-fin evaporators. Appl. Therm. Eng. 31, 2616–2621.
Silva, D.L., Melo, C., Hermes, C.J.L., 2017. Effect of frost morphology on the thermal-hydraulic performance of fan-supplied tube-fin evaporators. App. Therm. Eng. 111, 1060–1068.
Sommers, A.D., Truster, N.L., Napora, A.C., Riechman, A.C., Caraballo, E.J., 2016. Densification of frost on hydrophilic and hydrophobic substrates – Examining the effect of surface wettability. Exp. Therm. Fluid Sci. 75, 25–34.
Sommers, A.D., Gebhart, C., Hermes, C.J.L., 2017a. A study of frost growth on hydrophilic and hydrophobic surfaces under natural convection: a new semi-empirical correlation. Transfer Submitted to journal.
Sommers, A.D., Napora, A.C., Truster, N.L., Caraballo, E.J., Hermes, C.J.L., 2017b. A semi-empirical correlation for predicting the frost density on hydrophilic and hydrophobic surfaces. Int. J. Refrigeration 74, 311–321.
Tao, Y.X., Besant, R.W., Mao, Y., 1993. Characteristics of frost growth on a flat plate during the early growth period, ASHRAE Transactions: Symposia, CH-93-2-2 746–753.
Yonko, J.D., Sepsy, C.F., 1967. An investigation of the thermal conductivity of frost while forming on a flat horizontal plate. ASHRAE Trans. 2043, I1.1–I1.9.